Journal of Soil Science, 1983, **34**, 163–182

Pyrite and siderite oxidation in swamp sediments

DIEKE POSTMA

Institute of General Geology, Øster Voldgade 10, DK-1350 Copenhagen K, Denmark

Summary

Differences in the processes of pyrite and siderite oxidation, in reclaimed swamp sediments of the Skjernå delta (Denmark), are described from sediment chemistry, mineralogy and pore water chemistry.

Pyrite oxidation leads to extreme soil acidification, with pH dropping to about 2, the release of large amounts of weathering products to the pore water, and the precipitation of iron oxides, jarosite and gypsum.

Siderite oxidation results only in moderate soil acidification where the pH does not drop below 3.5, while part of the acidification is due to the oxidation of small amounts of sulphur compounds together with siderite. The release of weathering products to the pore water is limited and only iron oxide is precipitated.

Calculations indicate that equilibrium with amorphous FeOOH, gypsum and amorphous $Al(OH)_3$ sets an upper limit to the Fe^{3+}, SO_4 and Al concentrations in the pore water.

Introduction

Oxidation of Fe(II) compounds in soils, caused by reclamation and drainage of lowlands, is often a source of both agricultural and environmental problems. Agricultural problems include the acidification of soils and blocking of field drains by ochre (e.g. Bloomfield & Coulter, 1973; van Breemen, 1976). Environmental problems may arise when the drainwater is released into streams, due to low pH and/or ochre content, which have been documented especially for acid mine drainage (e.g. Sykora *et al.*, 1975; Tomkiewicz & Dunson, 1977).

Most of these problems are traditionally related to the oxidation of iron sulphides, in particular of pyrite. However, pyrite is not the only Fe(II) compound that may accumulate in anaerobic sediments, although it is certainly the most important. Under suitable conditions, siderite ($FeCO_3$) instead of pyrite may form in quantitatively significant amounts in anaerobic sediments (Postma, 1977, 1982). Since the effects of siderite oxidation are very different from pyrite oxidation, it is important for proper soil treatment to know whether pyrite or siderite is the dominant iron mineral.

In the swamp sediments of the Skjernå delta, Denmark, both pyrite and siderite are found in large amounts and spatially well separated. The distribution and conditions of formation for the two minerals have been discussed in a previous paper (Postma, 1982).

It was found that siderite occurs associated with fresh-water sediments in the

0022-4588/83/0300-0163 $02.00

eastern parts of the delta, while pyrite was found in the brackish water sediments of the western parts of the delta.

Reclamation of the area in the late sixties has resulted in a lowering of the water table which has accelerated oxidation processes in the upper layers of the deposit. The present report will focus on these oxidation processes with particular reference to the oxidation of pyrite and siderite.

Methods

The methods used for sampling and chemical analysis have for the major part been described by Postma (1981, 1982) and are summarized only briefly here.

In short, two types of borings have been made. The first type has the purpose of obtaining information on the distribution of iron and sulphur containing minerals in the deposit, both spatially throughout the delta and vertically in oxidized and reduced parts of the sediments. The boundary layer between oxidized and reduced sediments, here called the redoxcline, was determined by measuring pH and Eh profiles in the field. pH/Eh measurements were carried out with a portable pH-meter, inserting the electrodes directly into the sediment immediately after core recovery. The sediment samples were frozen in the field, in order to prevent oxidation, and transported in this state to the laboratory. The samples were subsequently freeze-dried and used for chemical analysis and X-ray diffraction. Total S and C were determined using a LECO induction furnace, while total Fe and other metals were analysed, as *aqua regia* soluble material, by flame AAS. SO_4-S was determined gravimetrically as $BaSO_4$ in sediment extracts obtained by boiling in 20% HCl (v : v). For further details, see Postma (1982).

The second type of boring was aimed at supplying information on the pore water chemistry of the deposit. The pore water was extracted with a Reeburgh (1967)-type sediment squeezer through 0.45 μm membrane filters. In order to prevent oxidation and degassing of the pore water samples, both pore water extraction and analysis for components sensitive to oxidation were carried out in the field in a nitrogen-filled glove box immediately after core recovery. Within the glove box, pH was measured, alkalinity was titrated and reagents added for colorimetric analysis of H_2S, Fe^{2+} and PO_4-P. In the laboratory, total dissolved Fe, Ca, Mn, Mg and Al were determined by flame AAS (flameless AAS for low Al concentrations) and Na and K by flame emission. High SO_4 concentrations were determined gravimetrically, while low SO_4 concentrations and Cl were analysed colorimetrically. For further details see Postma (1981).

Tritium contents in the pore water of one of the borings were determined by the Danish Isotope Centre (Copenhagen).

Supplementary information on pore water chemistry was obtained from permanently installed filters in the sediment, from which pore water samples were withdrawn periodically by suction. These samples will be referred to as filter samples. The equipment used is described by Nielsen & Postma (1980). All handling and analysis of samples sensitive to oxidation was again done in a nitrogen-filled glove box by similar procedures as for pore water samples. The filter samples were filtered through 0.1 μm membrane filters.

The activities of the ionic species and the saturation state of the pore water for different minerals, were calculated with a modified version of the computer program

WATEQF (Plummer *et al.*, 1976), the FORTRAN IV version of the original WATEQ program of Truesdell & Jones (1974).

One of the most important modifications of WATEQF was the treatment of redox reactions. For handling redox reactions, the input of WATEQF may either be measured Eh or a calculation of Eh from dissolved oxygen or SO_4/H_2S ratios. The input for iron is total Fe and the distribution between dissolved Fe(II) and Fe(III) species is calculated from Eh data. In particular, where significant amounts of dissolved Fe(III) are found, as here, it appears to be more realistic to use analytical data for Fe(II) and Fe(III) as the input for WATEQF. Fe(III) is here defined as the difference between total dissolved Fe (less than 0.45 or 0.1 μm) and Fe(II). WATEQF was therefore modified in order to allow input of Fe(II) and Fe(III) as a separate option. This was accomplished by setting up mass balance and mass action equations, separately for Fe(II) and Fe(III) species, in the same way as WATEQF treats other ionic species.

Other modifications of the original WATEQF program include the incorporation of new complexes, such as $Fe(SO_4)_2^-$ and $FeH_3SiO_4^{2+}$, and of new minerals like jarosite, natrojarosite, hydronium-jarosite and several others.

Activities were calculated from molar concentrations with the Davies equation (Stumm & Morgan, 1970). Temperatures of pore water samples ranged from 6 to 17°C but are for convenience set to 10°C in all calculations.

Dissociation constants for ion pairs, employed in WATEQF, were for hydroxy species taken from the compilation by Baes & Mesmer (1976). All sulphate complexes have been adopted from Nordstrom (1977). The dissociation constant of the $FeH_3SiO_4^{2+}$-complex is from Reardon (1979). Other constants of interest for this study, are similar to the Truesdell & Jones (1974) compilation. Dissociation constants for minerals will be referred to when encountered.

Results

Sediment composition

In the reduced parts of the Skjernå delta swamp sediments, pyrite and siderite are found in well-separated layers. Only in a very few samples were both minerals identified. In the near surface sediments, the occurrence of pyrite and siderite can be delineated as two provinces (Fig. 1) corresponding respectively to fresh and brackish water sediments (Postma, 1982).

Pyrite is found in the western parts of the peat basin and is present in large amounts. This is reflected by the chemical composition of the sediments (Fig. 2a), where below the redoxcline high concentrations of both aqua-regia-soluble-iron and total sulphur are found. It was shown (Postma, 1982) that, in general, sulphur and iron contents in the reduced zone of the western parts of the peat basin corresponded to the theoretical ratio in pyrite, and are therefore assumed to be largely present as pyrite. Pyrite has also been identified by X-ray diffraction. Sulphur concentrations range in the reduced zone mostly between 2 and 12% S dry wt, although values as high as 19% S dry wt have been measured.

The position of the redoxcline in the sediment sequence is reflected by an sharp increase of Eh and a corresponding drop of pH (Fig. 2a). In the oxidized zone, field observations indicated the presence of jarosite and iron oxide. X-ray diffraction confirmed the presence of jarosite and showed that gypsum is also present. Jarosite

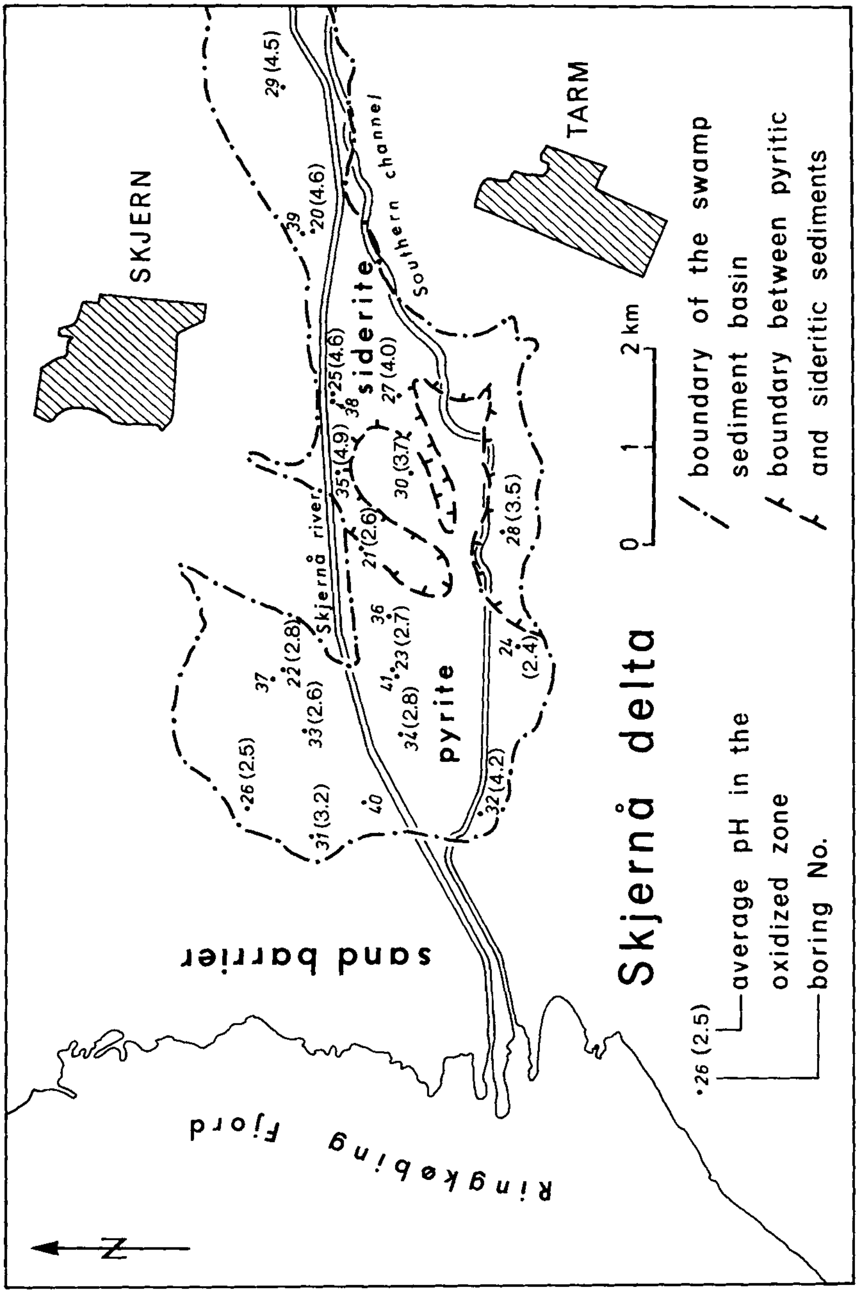

Fig. 1. The distribution of pyrite and siderite in the upper 2 m of the swamp sediments of the Skjernå delta (Denmark), slightly modified after Postma (1982). Superimposed is the measured average pH in the oxidized zone for each boring.

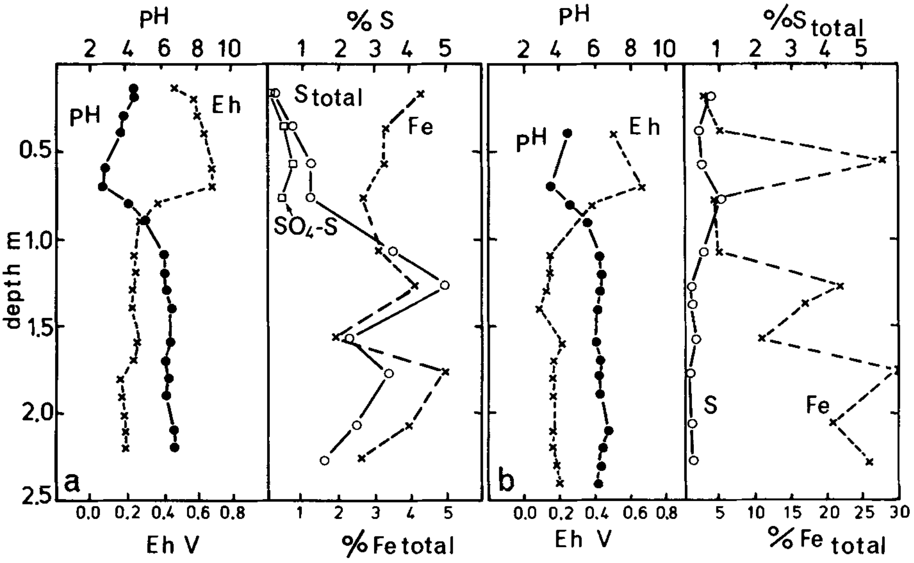

Fig. 2. Sulphur and iron contents related to pH/Eh in (a) pyritic sediments (boring 30) and (b) sideritic sediments (boring 25). Concentrations are expressed as % dry weight. Iron contents refer to *aqua regia* soluble Fe. For location see Fig. 1.

$(KFe_3(SO_4)_2(OH)_6)$ may occur in an almost complete range of solid solution with natrojarosite and hydronium-jarosite, where Na^+ and H_3O^+ are replacing K^+, although a strong preference for K^+ is found (van Breemen, 1976).

The extent of substitution of Na^+ and H_3O^+ for K^+ in the jarosite of Skjernå delta sediments is not known. It cannot be determined from X-ray diffraction data alone, and due to small grain sizes it is not possible to isolate the jarosite in pure form from the sediment for chemical analysis.

At the transition from the reduced to the oxidized zone (Fig. 2a), a significant fall in total sulphur concentration is observed, while iron remains roughly constant. In all borings of the pyritic area, a big increase of the Fe/S ratio was observed above the redoxcline. Sulphur in the oxidized sediments is mostly present as sulphate (Fig. 2a), probably mainly as gypsum and jarosite. It appears that the dominant part of the iron released by pyrite oxidation remains *in situ* as iron oxides and jarosite, while the major part of pyrite sulphur after oxidation is transported away as dissolved sulphate leaving only minor amounts as gypsum and jarosite.

Siderite is found in the reduced sediments of the eastern part of the peat basin, and often occurs together with small amounts of vivianite. Both minerals have been identified by X-ray diffraction. The iron content of the sideritic sediments is also very high (Fig. 2b). Although there is a tendency towards higher iron contents in the sideritic sediments than in the pyritic sediments, the large difference in iron content displayed in Figs 2(a) and 2(b) is accidental. Iron contents of up to 30% Fe dry wt have been measured in sideritic sediments, against 19% Fe dry wt in the pyritic sediments.

Chemical analysis (Postma, 1982) has shown that the major part of the iron in the reduced zone of sideritic sediments is present as siderite and vivianite. The low total sulphur contents (Fig. 2b) demonstrate that the pyrite content of the sideritic sediments must be very low.

The position of the redoxcline is again indicated by a sharp increase of Eh and a corresponding decrease of pH. The iron content of the sediment varies considerably with depth (Fig. 2b). Generally, there is no significant difference between the iron content of the oxidized and the reduced zone. Iron is mainly present as iron oxide in the oxidized zone. It appears that most iron released by siderite oxidation remains *in situ* as iron oxide. Attempts to identify specific iron oxide minerals by X-ray diffraction failed, probably due to the poor crystallinity of the material. Minerals like gypsum and jarosite, which were observed in pyritic sediments, were never found in sideritic sediments.

pH and Eh distribution

The thermodynamic significance of Eh measurements in natural environments is usually highly questionable (e.g. Doyle, 1968; Stumm & Morgan, 1970), although there is little doubt that oxidized sediments yield high Eh and reduced sediments low Eh values. It was therefore decided not to interpret the measured Eh values in an absolute sense, but rather to use the shape of the Eh profiles for determination of the position of the redoxcline in the sediments. Fig. 2 shows that the transition between high Eh values in the oxidized zone and lower values in the reduced zone is very distinct, and allows an accurate location of the redoxcline. Generally, the position of the redoxcline is between 50 and 100 cm below the surface.

pH measurements in the reduced zone show no significant differences between pyritic and sideritic sediments. There is also very little pH variation with depth and the major part of the pH measurements fall within the range 6–7.

In the oxidized zone, there is a marked difference in pH between pyritic and sideritic sediments. In the pyritic sediments, pH values as low as 1.8 have been measured and values between 2 and 3 are common (Figs 2a and 4). In the sideritic sediments, pH values do not reach such low values, and are 3.5 and above (Figs 2b and 9). The association of lower pH values in the pyritic sediments, compared to sideritic sediments, is also illustrated in Fig. 1. Here, average pH values from the oxidized parts of the borings are shown superimposed on a distribution map of pyrite and siderite in the near surface layers of the sediments. It is obvious from Fig. 1 that the pH measured in the oxidized zone is closely related to the presence of pyrite and siderite in the underlying sediments.

Hydrology

Variations of the groundwater table were measured over a period of 13 months at three localities (near borings 36, 40 and 25 in Fig. 1). For all three localities there was a high water table, close to the sediment surface, from November to March, and during summer months a lower water table, generally between 0.5 and 1.0 m below the sediment surface.

For evaluation of the vertical water transport, the pore water from boring 36 was dated by its tritium content. [^{3}H]tritium was released to the atmosphere in considerable amounts by nuclear weapon testing during the late fifties and the start of the sixties. Prenuclear tritium contents in rain-water were of the order of a few T.U.

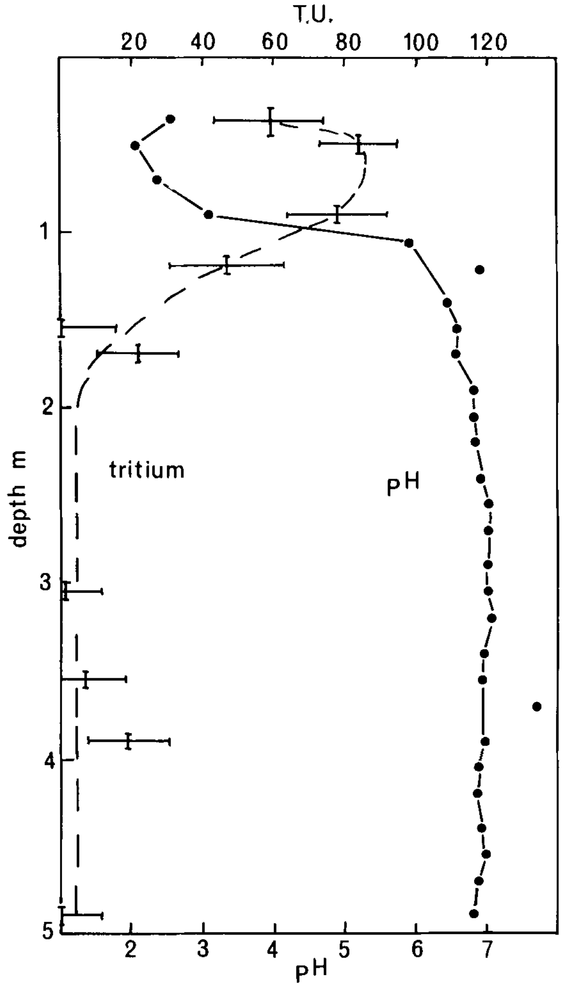

Fig. 3. Tritium contents in the pore waters of boring 36. 1 T.U. corresponds to 1 tritium atom per 10^{18} hydrogen atoms. The redoxcline is located at the sharp decrease of pH.

(1 T.U. = 1 tritium atom per 10^{18} hydrogen atoms), and a sharp maximum of tritium input is found around 1963 (e.g. Imboden *et al.*, 1977).

Results for tritium contents in the pore water of boring 36 are shown in Fig. 3, together with the pH profile for comparison. The sharp increase of pH at about 1 m depth corresponds to the redoxcline. Fig. 3 shows that while relatively high tritium contents are found in the oxidized zone, tritium contents decrease very rapidly in the reduced zone and approach zero at a depth of only 2 m. Since the tritium-free water dates pre-1960, it must be concluded that replacement of water in the reduced zone is of minor importance in the water balance.

Pore water chemistry

An example of the pore water chemistry of the pyritic area is shown in Fig. 4. In the oxidized zone, pH is very low with values down to about 2.

The high concentrations of iron and sulphate in the pore water indicate active pyrite oxidation. Note that the iron and sulphate concentrations here roughly correspond to the molar Fe/S ratio in pyrite. In other borings, however, large deficits of iron relative to sulphate have been observed. In the oxidized zone Fe(II) constitutes only a minor part of total dissolved iron (<0.45 µm) (Fig. 5). The proportion of Fe(II) to total dissolved iron is, however, highly variable.

Sulphate released by pyrite oxidation is transported down along the concentration gradient into the underlying sediments to a maximum depth of about 4 m (Fig. 6).

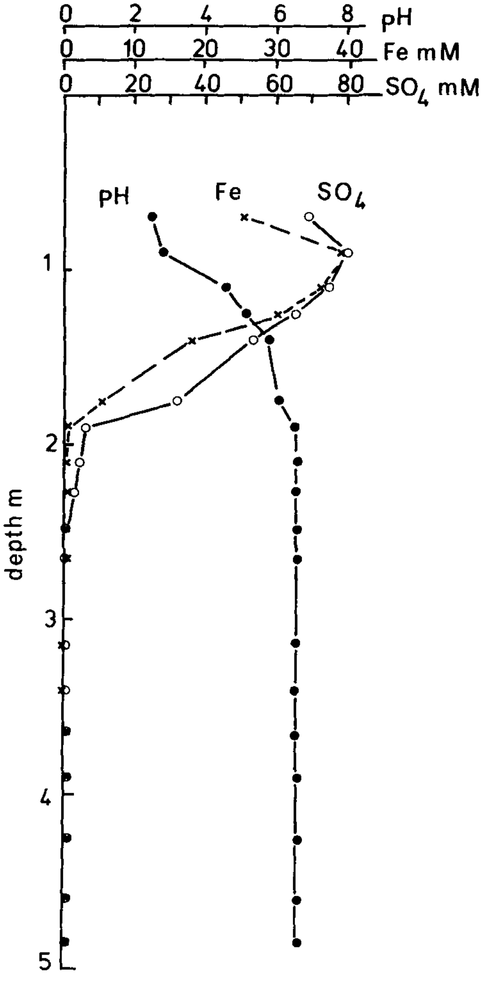

Fig. 4. Pore water composition of pyritic sediments in boring 41. Iron concentrations are total dissolved Fe (<0.45 µm).

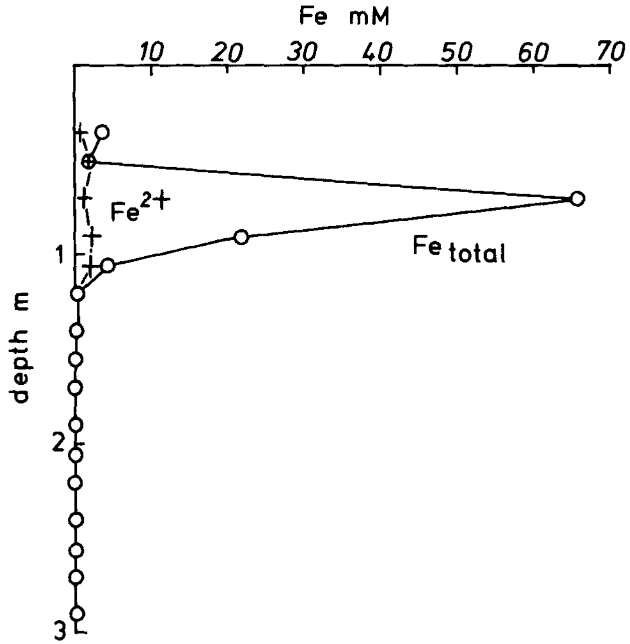

Fig. 5. Total dissolved Fe (<0.45 μm) and Fe(II) in pore waters of pyritic sediments (boring 36). The redoxcline is located at 1 m depth.

Below the redoxcline, sulphate is reduced again, as shown by the appearance of H_2S in the pore waters of some borings (Postma, 1982).

Sulphate reduction also causes an increase of alkalinity (e.g. Berner *et al.*, 1970; Sholkovitz, 1973). This is illustrated in Fig. 7, where sulphate is plotted against alkalinity, using part of the data from borings 36 and 37. The contribution of bacterial ammonia production to the alkalinity (Berner *et al.*, 1970), which amounts to one equivalent of HCO_3^- for each mole of NH_4^+ produced, has been subtracted from the plotted alkalinity values.

The low pH in the oxidized zone causes the disintegration of silicates, as demonstrated by the high concentrations of aluminia and silica found in the oxidized zone (Fig. 8). Also, magnesium and calcium are strongly enriched in the oxidized zone.

The pore water chemistry of the sideritic area is illustrated in Fig. 9. The effects of oxidation are here less dramatic than in the pyritic area. pH is lowest in the oxidized zone, but remains above 3.5.

There are again enrichments of iron and sulphate in the oxidized zone, but concentrations are less than in the pyritic area (note the difference in scale between Figs 4 and 9). The moderate sulphate concentrations indicate that apart from siderite oxidation, oxidation of small amounts of iron sulphide or organic sulphur compounds also occurs. This is in agreement with the presence of small amounts of sulphur in the sideritic sediments. Dissolved iron is here found to penetrate much deeper into the reduced sediments, compared with the pyritic sediments where most of the dissolved iron is precipitated as iron sulphide. In the oxidized zone iron contents are generally low, with very little Fe(III) in solution due to a higher pH. The

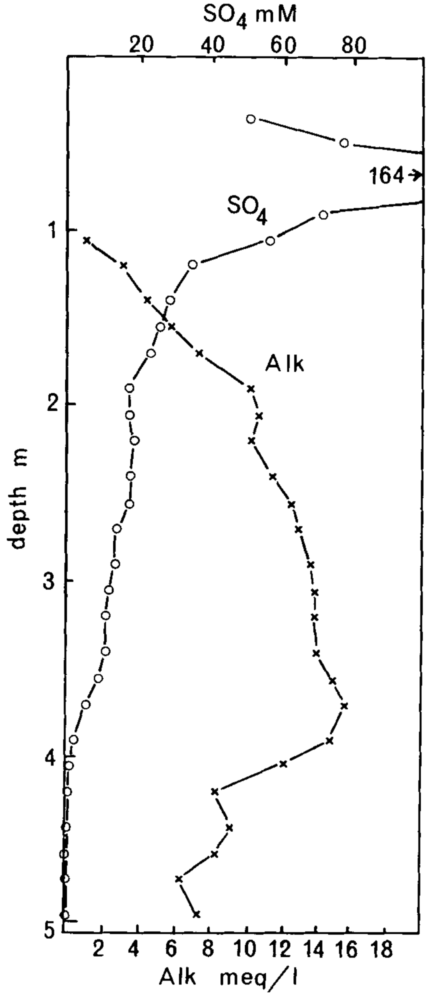

Fig. 6. Sulphate and alkalinity in pore waters of pyritic sediments of boring 36. The redoxcline is at 1 m depth.

higher pH in the oxidized zone of the sideritic sediments causes only limited weathering of silicates. Slight enrichments of aluminium and silica are found, but are quite insignificant compared with the pyritic sediments.

Discussion

Pyrite oxidation

The overall stoichiometry for complete pyrite oxidation is:

$$FeS_2+\frac{15}{4}O_2+\frac{5}{2}H_2O \rightarrow FeOOH+2SO_4^{2-}+4H^+ \qquad (1)$$

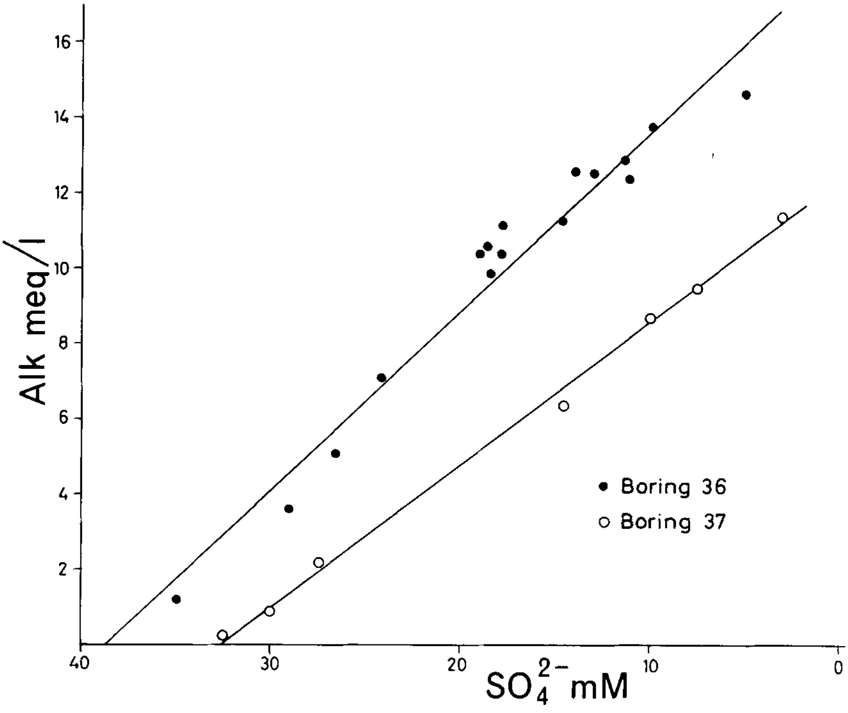

Fig. 7. Sulphate decrease versus alkalinity increase, in pore waters of pyritic sediments. Alkalinity values are corrected for alkalinity resulting from NH_4 formation. Data shown for boring 36 is from the depth interval 115–375 cm below the surface. Also included are data from boring 37, depth interval 85–195 cm below the surface.

Mechanisms of pyrite oxidation have been reviewed in several papers (Bloomfield & Coulter, 1973; van Breemen, 1973*a*; Dent & Raiswell, 1982) and will not be repeated in detail here. Generally, fast pyrite oxidation proceeds through oxidation of FeS_2 by Fe^{3+} (Garrels & Thompson, 1960; Smith *et al*., 1968; Singer & Stumm, 1970) and requires a low pH since Fe(III) is otherwise insoluble. Oxygen enters the process by oxidizing Fe(II) to Fe(III). At low pH the oxidation rate of Fe(II) is inorganically very slow, but under field conditions the process is strongly catalysed by bacteria like *Thiobacillus ferrooxidans* (e.g. Schnaitman *et al*., 1969; Stumm-Zollinger, 1972).

Intensive pyrite oxidation in the sediments of the Skjernå delta is reflected by a low pH, the high concentrations of iron and sulphate in the pore waters, and the presence of oxidation products like jarosite and gypsum. Field pH measurements in the oxidized zone of the Skjernå delta sediments are often between 2 and 3, while van Breemen (1976) only reported field measurements higher than 3. The lower pH values found here suggests very high pyrite oxidation rates, but could partly be due to poor buffering properties of the Skjernå delta sediments.

It has been found from experimental work that the oxidation of Fe(II) by oxygen is rate limiting in the total process of pyrite oxidation when abundant O_2 is present

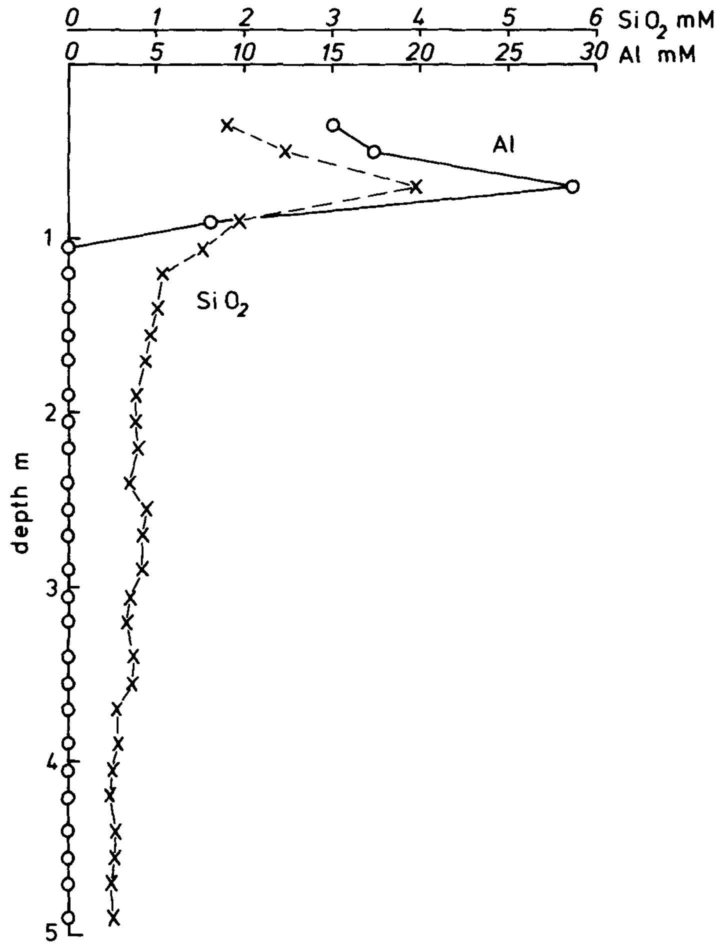

Fig. 8. Products of silicate weathering in pore waters of pyritic sediments of boring 36. The redoxcline is at 1 m depth.

(Singer & Stumm, 1970; Stumm-Zollinger, 1972). It is, however, questionable whether this also is true under field conditions. Most authors (Rasmussen, 1961; van Breemen, 1976; Dent & Raiswell, 1982) agree that under field conditions, diffusion of oxygen into the soil is rate limiting in the total process of pyrite oxidation. In consequence, very little Fe(III) should be present in the pore water.

In the Skjernå delta sediments, however, significant amounts of Fe(III) were measured in the pore waters of the oxidized zone (Fig. 5). These measurements reflect mainly periods with a high watertable, because the porewater of the oxidized zone could not be sampled during periods with a low watertable. If oxygen diffusion is rate limiting, the high Fe(III) concentrations in the pore water cannot be a direct result of pyrite oxidation. More likely, the high Fe(III) concentrations are due to dissolution of oxidation products like jarosite and iron oxyhydroxides which have accumulated during the previous dry period.

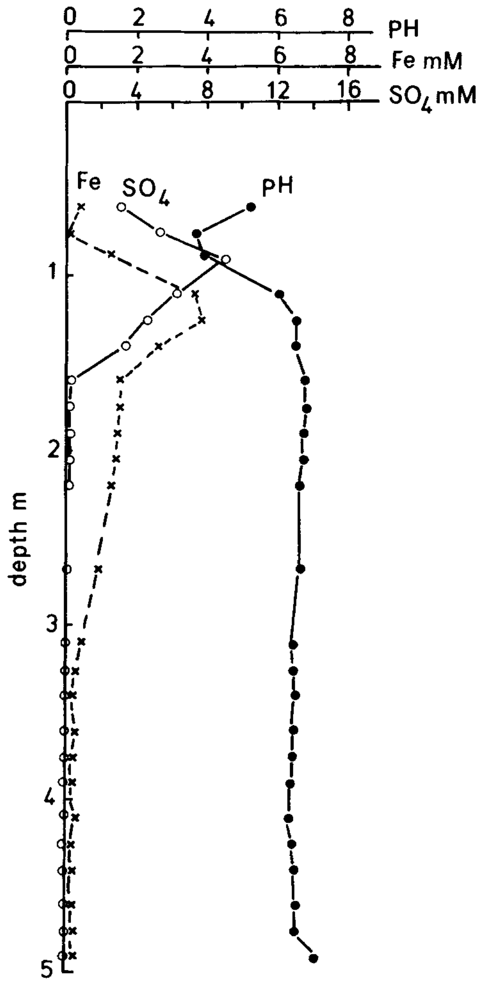

Fig. 9. Pore water composition of sideritic sediments in boring 38. Total dissolved Fe (<0.45 μm) are the same as Fe(II) concentrations in this boring. Note the difference of scale with Fig. 4.

The very low pH in the oxidized zone allows the solution of considerable amounts of Fe(III). A secondary effect of this process is that the released Fe(III) becomes available for continued oxidation of pyrite during periods with a high water-table (van Breemen, 1976).

Siderite oxidation

For oxidation of siderite we may write an overall reaction as:

$$2FeCO_3+0.5O_2+3H_2O \rightarrow 2FeOOH+2H_2CO_3 \qquad (2)$$

The production of carbonic acid by this reaction should decrease pH. If reaction (2) is the only one that takes place, the resulting pH can be estimated from the relation (van Breemen, 1975):

$$pH = 0{\cdot}5(pK_{CO_2} + pK_l) - 0{\cdot}5 \log P_{CO_2} \quad (3)$$

Here, K_{CO_2} and K_l refer to Henry's law and the first dissociation constant for carbonic acid. For 10°C the expression is:

$$pH = 3.87 - 0.5 \log P_{CO_2} \quad (4)$$

For a realistic range of P_{CO_2} from 10^{-1} to 10^{-3} atm, the resulting pH should vary between 4.4 and 5.4. Since Fe(III) in this pH range is still very insoluble ($a_{Fe3+} \sim 10^{-7}$ M), the oxidation of siderite should not bring significant amounts of Fe(III) in solution. The low iron concentrations in the pore water of oxidized sideritic sediments (Fig. 9) confirm this.

Measured pH values in the oxidized zone of sideritic sediments range from 3.5 to 5.5 with an average around 4.5 and are thus slightly lower than theoretically estimated. The deviation may be due to oxidation of some iron sulphide or organic sulphur compounds which contributes to acid production. Acid production from sulphide oxidation is much larger than that of siderite oxidation.

Field observations as well as theoretical arguments therefore support the conclusion that siderite oxidation causes only a moderate acidification of the soil, while most of the iron remains *in situ* as iron oxides and only very little iron is released to the pore water.

Oxidation products and pore water chemistry

The concentrations of oxidation products from pyrite and siderite in the pore waters depend not only on the release from the original minerals, but also on the precipitation of new minerals, weathering of silicates and lateral transport. Controls on the pore water chemistry by precipitation of oxidation products might to some extent be evaluated by comparing the activity products in the pore water with the solubility constants for the minerals involved.

Common to both siderite and pyrite oxidation is the formation of iron oxyhydroxides and these should be expected to control the Fe(III)-concentrations in the pore water.

The iron oxyhydroxides cover a wide range of stability, from freshly precipitated amorphous material, here described as $Fe(OH)_3$, to coarsely crystalline goethite, corresponding respectively to solubilities from −37.1 to −44.2 (at 25°C for $\log K = \log a_{Fe3+} + 3\log a_{OH^-}$) Langmuir & Whittemore, 1971; Whittemore & Langmuir, 1975).

The solubility of the least and most soluble iron oxyhydroxide are given as the solid lines in Fig. 10, together with the calculated values for α_{FE3+} and α_{OH^-} of the pore water from the oxidized zone. Most of the pore water data in Fig. 10 is from pyritic sediments, since in sideritic sediments the difference between analytical concentrations of Fe_{total} and Fe(II) with few exceptions is insignificant.

Fig. 10 shows that the pore water from the oxidized zone is greatly supersaturated with respect to goethite and is closer to equilibrium with $Fe(OH)_3$. This suggests that equilibrium with $Fe(OH)_3$ controls the maximum α_{Fe3+} in the pore water, rather than more stable forms of iron oxyhydroxides.

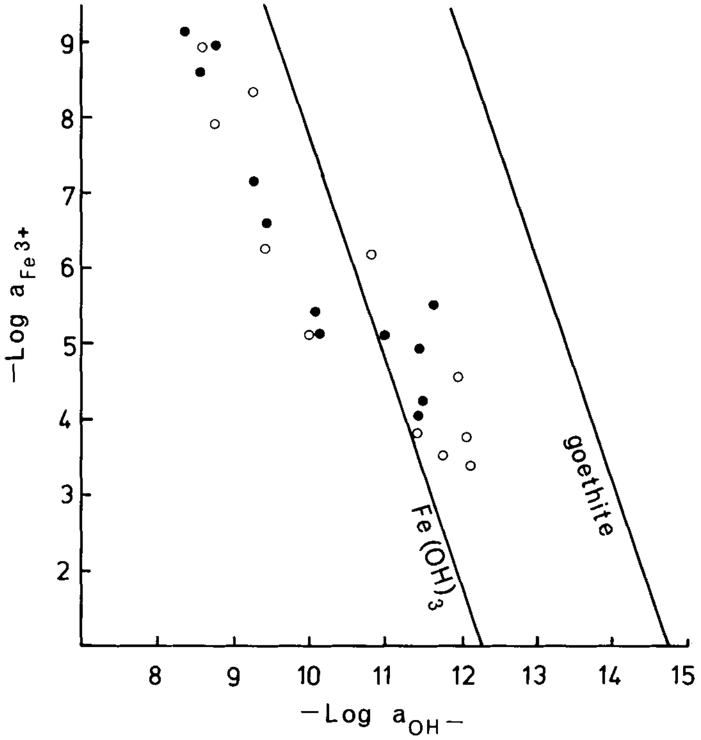

Fig. 10. The saturation state of the pore water for iron oxyhydroxides. Fe(OH)$_3$ refers to freshly precipitated material (pK = 37.8 at 10°C) and goethite to coarsely crystalline goethite (pK = 45.2 at 10°C) (Whittemore & Langmuir, 1975). Open circles refer to pore water samples (squeezed and filtered through 0.45 μm) and closed circles to filter samples (taken by suction and filtered through 0.1 μm).

There is in Fig. 10 a tendency towards supersaturation in the higher pH range. It is not clear whether this might be due to an analytical underestimation of Fe(II) resulting in too high Fe(III) concentrations. In this pH range the oxidation of Fe^{2+} is very fast (Stumm & Morgan, 1970), but drastic precautions to prevent oxidation were taken and no precipitation of iron oxides was observed during sample handling in the glove box.

One possibility is that total dissolved iron includes particulate material. Pore water and filter samples, were filtered through 0.45 and 0.1 μm filters respectively and these two sets of data do not show any consistent difference in saturation state (Fig. 10). Thus, if particulate iron contributes significantly to the total dissolved iron concentration, it should have a grain size of less than 0.1 μm.

It should also be emphasized that for calculating the $a_{Fe^{3+}}$, the effect of ion pairing is extremely important. 'Free' Fe^{3+} concentrations are about 10% of total dissolved Fe(III) in the lower pH range of Fig. 10, but in the higher pH range their contribution may drop below 0.01%. Since activities are roughly a magnitude lower than molar concentrations, the displayed $a_{Fe^{3+}}$ is only a very small fraction of the analytical Fe(III) concentration.

An alternative constraint on the dissolved Fe(III) concentration could, at least in pyritic sediments, be the precipitation of jarosite. Jarosite was found in the most acid (pH 1.8–3.0) pyritic sediments, in good agreement with the instability of jarosite with respect to iron oxyhydroxides towards higher pH (van Breemen, 1976) although jarosite may persist metastably at higher pH (Dent, 1980). Several authors (van Breemen, 1976; Nordstrom *et al.*, 1979) have reported extremely high degrees of supersaturation in acid sulphate waters for pure jarosite (up to eight orders of magnitude!). Also in this study very high degrees of supersaturation are found for both jarosite and natrojarosite, while for hydronium-jarosite undersaturation prevails. Naturally occurring jarosite is, however, a solid solution of jarosite, natrojarosite and hydronium-jarosite with unknown composition and solubility. Calculated saturation states for pure end members provide therefore little information on the actual saturation state of the pore water for the jarosite found in the sediment.

An alternative constraint on the sulphate concentrations in the pore waters could be the precipitation of gypsum. Gypsum has frequently been found in the oxidized zone of the pyritic sediments. The saturation state of the pore water for gypsum is, for two borings of the pyritic area, shown in Fig. 11. The dissociation constant for gypsum has a value of $\log K = -4.60$ at 25°C or -4.62 at 10°C (Wigley, 1973). It might be seen that the pore water in the oxidized zone is very close to saturation in the upper parts and weakly supersaturated in the lower parts, where pyrite oxidation is most intensive. In the reduced zone, the pore water becomes undersaturated as expected. The near equilibrium of the pore water from the oxidized zone, together with the actual occurrence of gypsum here, are good arguments for an equilibrium control of both $a_{Ca^{2+}}$ and $a_{SO_4^{2-}}$. Also van Breemen (1976) and Nordstrom (1977) have observed that equilibrium with gypsum gives an upper limit for Ca^{2+} and SO_4^{2-} activities. In the oxidized zone of sideritic sediments the pore water is always strongly undersaturated for gypsum, in good agreement with the absence of gypsum here.

The acid production, caused by pyrite oxidation, gives rise to silicate weathering as reflected by the high SiO_2 and Al concentrations in the pore waters of the oxidized zone (Fig. 8).

The most probable mechanism by which aluminium could be removed from solution is precipitation of gibbsite or amorphous $Al(OH)_3$ (Frink, 1973). The mineral gibbsite could not be identified in the sediments by standard X-ray diffraction methods, but may be present in small amounts or as X-ray-amorphous material.

The gibbsite equilibrium is described by the reaction:

$$Al(OH)_3 \rightleftharpoons Al^{3+} + 3OH^- \tag{5}$$

The solubility constant for gibbsite, according to reaction (5), was taken from a recent critical evaluation by Hemingway *et al.* (1978) where $\log K = -33.91$ at 25°C or -34.58 at 10°C. Reported values for cryptocrystalline or amorphous $Al(OH)_3$ at 25°C, also for reaction (5), are -32.65 (Hem & Roberson, 1967) and -32.77 (Helgeson, 1969). Using Hem and Roberson's value for K and the heat of reaction from Helgeson, $\log K = -33.27$ at 10°C.

The activities of Al^{3+} and OH^-, for pore water samples from the oxidized zone and the top of the reduced zone, were plotted in a stability diagram for gibbsite and amorphous $Al(OH)_3$ (Fig. 12). The samples with the highest $a_{Al^{3+}}$ and the lowest pH, are undersaturated for both forms of $Al(OH)_3$. With increasing pH the pore

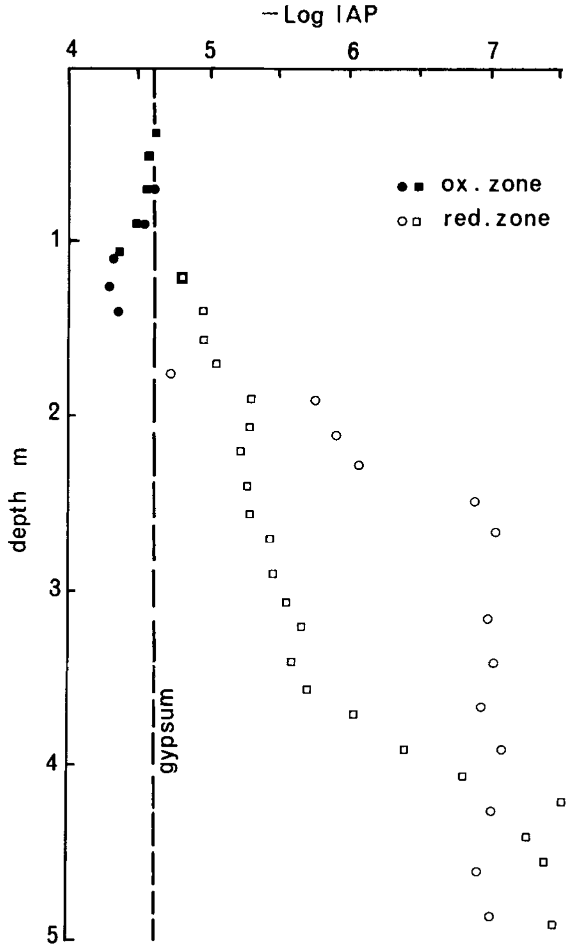

Fig. 11. The saturation state (log IAP = log $a_{Ca^{2+}}$ + log $a_{SO_4^{2-}}$ + log a_{H_2O}) of pore waters from pyritic sediments for gypsum. Squares, boreing 36; circles, boring 41.

water becomes supersaturated for gibbsite and equilibrium with amorphous $Al(OH)_3$ is approached.

Of the two data sets, the filter samples are closest to equilibrium with amorphous $Al(OH)_3$, while pore water samples show a tendency towards supersaturation. The major difference between these two sets of data, is that pore water samples have been filtrated through 0.45 µm and filter samples through 0.1 µm membrane filters. Kennedy *et al.* (1974) and Busenberg & Clemency (1976) showed that 0.45 µm filters, in contrast to 0.1 µm filters, may yield Al results which are too high. This may explain the difference between the two data sets in Fig. 12. Kennedy *et al.* noted the same effect for Fe, but this is not apparent from Fig. 10.

The data presented in Fig. 12 suggest that equilibrium with amorphous $AL(OH)_3$ controls the maximum $a_{Al^{3+}}$ in solution. Experimental work has shown that the formation of crystalline gibbsite from aqueous solution is a very slow process requiring equilibration times as long as 400–600 days (Hemingway *et al.*, 1978). With

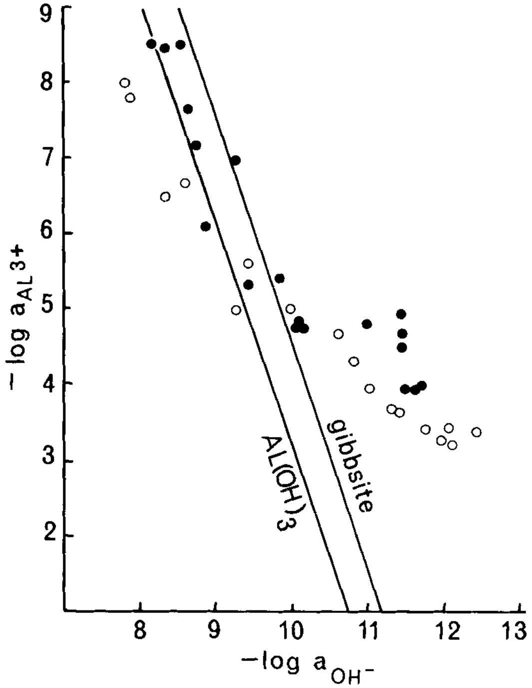

Fig. 12. The saturation state of pore waters from the oxidized zone of pyritic sediments for gibbsite. $Al(OH)_3$) represents amorphous material or cryptocrystalline gibbsite. Pore water samples are displayed as open circles and filter samples as filled circles (for explanation see Fig. 10).

a continuous release of Al from silicate weathering, it is unlikely that equilibrium with crystalline gibbsite can be attained.

van Breemen (1973*b*, 1976) proposed that the $a_{Al^{3+}}$ in the pore waters of acid sulphate soils is controlled by a hypothetical compound of stoichiometric composition $AlOHSO_4$, because a near constant value of -17.35 for the activity product $\log a_{Al^{3+}} + \log a_{OH^-} + \log a_{SO_4^{2-}}$ was found in the pore waters.

The present data is especially below saturation for gibbsite in reasonable agreement with this hypothetical $AlOHSO_4$ as values for the activity product range from -16.74 to -18.69. The approach, however, of assigning an empirical ion activity product to an unknown hypothetical mineral, appears to be somewhat questionable. Experimental verification is clearly needed here.

Although gibbsite or amorphous $Al(OH)_3$ could not be identified either in the Skjernå delta sediments, the precipitation of $Al(OH)_3$ during silicate weathering is a better documented process. Experimental dissolution of feldspars (Busenberg & Clemency, 1976; Busenberg, 1978) as well as muscovite (Lin & Clemency, 1981), have shown that equilibrium with amorphous $Al(OH)_3$ controls the $a_{Al^{3+}}$ in solution. In addition, Busenberg (1978) identified a precipitate of X-ray amorphous $Al(OH)_3$ as a product of feldspar dissolution.

Experimental work supports therefore the field evidence which indicates that equilibrium with amorphous $Al(OH)_3$ or cryptocrystalline gibbsite imposes an upper limit to dissolved aluminium concentrations in the pore waters of the oxidized zone.

Acknowledgements

The efforts of Søren Nielsen, Ellen Zimmer and Lotte Nielsen during many field trips, made this project possible. Helpful reviews were given by Jens Jacobsen and Dave Rickard. Part of this work was done at the Geological Survey of Denmark. This project was granted financial support by the Danish Natural Science Research Council.

REFERENCES

Baes, C.F., Jr & Mesmer, R.E. 1976. *The Hydrolysis of Cations*. New York: Wiley Interscience.

Berner, R.A., Scott, M.R. & Tomlinson, C. 1970. Carbonate alkalinity in the porewaters of anoxic marine sediments. *Limnology and Oceanography* **15**, 544–549.

Bloomfield, C. & Coulter, J.K. 1973. Genesis and management of acid sulfate soils. *Advances in Agronomy* **25**, 265–326.

Breemen, N. van 1973*a*. Soil forming processes in acid sulphate soils In *Acid Sulphate Soils* (ed. H. Dost) International Institute for Land Reclamation and Improvement pub. 18, **1**, pp. 66–128.

Breemen, N. van 1973*b*. Dissolved aluminium in acid sulfate soils and in acid mine waters. *Proceedings Soil Science Society of America* **37**, 694–697.

Breemen, N. van 1975. Acidification and deacidification of coastal plain soils as a result of periodic flooding. *Proceedings Soil Science Society of America* **39**, 1153–1157.

Breemen, N. van 1976. *Genesis and Solution Chemistry of Acid Sulfate Soils in Thailand*. Pudoc, Wageningen.

Busenberg, E. 1978. The products of the interaction of feldspars with aqueous solutions at 25°C. *Geochimica et Cosmochimica Acta* **42**, 1679–1686.

Busenberg, E. & Clemency, C.V. 1976. The dissolution kinetics of feldspars at 25°C and 1 atm CO_2 partial pressure, *Geochimica et Cosmochimica Acta* **40**, 41–49.

Dent, D. 1980. Acid sulphate soils: morphology and prediction. *Journal of Soil Science* **31**, 87–99.

Dent, D. & Raiswell, R.W. 1982. Quantitative models to predict the rate and severity of acid sulphate development: a case study in The Gambia. In *Proceedings 2nd Symposium on acid sulphate soils* (ed. H. Dost). International Institute for Land Reclamation and Improvement, in press.

Doyle, R.W. 1968. The origin of the ferrous ion-ferric oxide Nernst potential in environments containing dissolved ferrous iron. *American Journal of Science* **266**, 840–859.

Frink, C.R. 1973. Aluminium chemistry in acid sulfate soils. In *Acid Sulphate Soils* (ed. H. Dost) International Institute for Land Reclamation and Improvement pub. 18. **I**, pp. 131–168.

Garrels, R.M. & Thompson, M.E. 1960. Oxidation of pyrite by iron sulfate solutions. *American Journal of Science* **258**, 57–67.

Helgeson, H.C. 1969. Thermodynamics of hydrothermal systems at elevated temperatures and pressures. *American Journal of Science* **267**, 729–804.

Hem, J.D. & Roberson, C.E. 1967. Form and stability of aluminium hydroxide complexes in dilute solution. U.S. Geological Survey Water Supply Paper 1827-A.

Hemingway, B.S., Robie, R.A. & Kittrick, J.A. 1978. Revised values for the Gibbs free energy of formation of $(\mathrm{Al(OH)}_{4\,aq}^{-})$, diaspore, boehmite and bayerite at 298. 15 K and 1 bar, the thermodynamic properties of kaolinite at 800 K and 1 bar, and the heat of solution of several gibbsite samples. *Geochimica et Cosmochimica Acta* **42**, 1533–1543.

Imboden, D.M., Weiss, R.F., Craig, H., Michel, R.L. & Goldman, C.R. 1977. Lake Tahoe geochemical study. 1. Lake chemistry and tritium mixing study. *Limnology and Oceanography* **22**, 1039–1051.

KENNEDY, V.C., ZELLWEGER, G.W. & JONES, B.F. 1974. Filter pore-size effects on the analysis of Al, Fe, Mn and Ti in water. *Water Resources Research* **10**, 785–790.

LANGMUIR, D. & WHITTEMORE, D.O. 1971. Variations in the stability of precipitated ferric oxyhydroxides. In *Non equilibrium systems in natural water chemistry* (ed. J. D. Hem) Advances in Chemistry Series (ACS) 106, 209–234.

LIN, F.C. & CLEMENCY, C.V. 1981. The kinetics of dissolution of muscovites at 25°C and 1 atm CO_2 partial pressure. *Geochimica et Cosmochimica Acta* **45**, 571–576.

NIELSEN, S. & POSTMA, D. 1980. An apparatus for temporal sampling without air contact of pore water from swamp sediments. Danmarks Geologiske Undersøgelse Årbog 1979, 31–39.

NORDSTROM, D.K. 1977. Hydrogeochemical and microbiological factors affecting the heavy metal chemistry of an acid mine drainage system. Ph.D. thesis, Stanford University.

NORDSTROM, D.K., JENNE, E.A. & BALL, J.W. 1979. Redox equilibria of iron in acid mine waters. In *Chemical modeling in aqueous systems* (ed. E. A. Jenne), ACS Symposium Series 93, 49–79.

PLUMMER, L.N., JONES, B.F. & TRUESDELL, A.H. 1976. WATEQF: A FORTRAN IV version of WATEQ, a computer program for calculating chemical equilibrium in natural waters. U.S. Geological Survey Water Resources Investigations 76–13.

POSTMA, D. 1977. The occurrence and chemical composition of recent Fe-rich mixed carbonates in a river bog. *Journal of Sedimentary Petrology* **47**, 1089–1098.

POSTMA, D. 1981. Formation of siderite and vivianite and the pore-water composition of a recent bog sediment in Denmark. *Chemical Geology* **31**, 225–244.

POSTMA, D. 1982. Pyrite and siderite formation in brackish and freshwater swamp sediments. *American Journal of Science*, in press.

RASMUSSEN, K. 1961. Uorganiske svovlforbindelses omsaetninger i jordbunden. Thesis Veterinaer og Landbohøjskolen, København.

REARDON, E.J. 1979. Complexing of silica by iron (III) in natural waters. *Chemical Geology* **25**, 339–345.

REEBURGH, W.S. 1967. An improved interstitial water sampler. *Limnology and Oceanography* **12**, 163–165.

SCHNAITMAN, C.A., KORCZYNSKI, M.C. & LUNDGREN, D.G. 1969. Kinetic studies of iron oxidation by whole cells of *Ferrobacillus ferrooxidans*. *Journal of Bacteriology* **99**, 552–557.

SHOLKOVITZ, E. 1973. Interstitial water chemistry of Santa Barbara Basin sediments. *Geochimica et Cosmochimica Acta* **37**, 2043–2073.

SINGER, P.C. & STUMM, W. 1970. Acidic mine drainage: the rate determining step. *Science* **167**, 1121–1123.

SMITH, E.E., SVANKS, K. & SHUMATE, K. 1968. Sulfide to sulfate reactions studies. *Second Symposium on Coal Mine Drainage Research. Pittsburgh*, 1–11.

STUMM, W. & MORGAN, J.J. 1970. *Aquatic chemistry*. New York: Wiley Interscience.

STUMM-ZOLLINGER, E. 1972. Die bakterielle Oxydation von Pyrit. *Archiv für Mikrobiologie* **83**, 110–119.

SYKORA, J.L., SMITH, E.J., SYNAK, M. & SHAPIRO, M.A. 1975. Some observations on spawning of brook trout (*Salvelinus fontinalis*, Mitchill) in lime neutralized iron hydroxide suspensions. *Water Research* **9**, 451–458.

TOMKIEWICZ, S.M. & DUNSON, W.A. 1977. Aquatic insect diversity and biomass in a stream marginally polluted by acid strip mine drainage. *Water Research* **11**, 397–402.

TRUESDELL, A.H. & JONES, B.F. 1974. WATEQ, a computer program for calculating chemical equilibria in natural waters. *U.S. Geological Survey Journal of Research* **2**, 233–248.

WHITTEMORE, D.O. & LANGMUIR, D. 1975. The solubility of ferric oxyhydroxides in natural waters. *Ground Water* **13**, 360–365.

WIGLEY, T.M.L. 1973. Chemical evolution of the system calcite-gypsum-water, *Canadian Journal of Earth Science* **10**, 306–315.

(*Received 22 July 1981*)